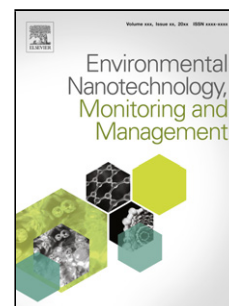


Journal Pre-proof

Synthesis of an Environmental Nano-Polyoxometalate ($\alpha_2\text{P}_2\text{W}_{17}\text{CoO}_{61}$)⁸⁻ As Catalyst for Dyes Degradation: A Comparative Study Oxidation of Indigoid And Azo dyes

Mohammed Grabsi, Nacéra Zabat, Nabila Khellaf, Fadhe Ismail



PII: S2215-1532(19)30183-7

DOI: <https://doi.org/10.1016/j.enmm.2019.100269>

Reference: ENMM 100269

To appear in: *Environmental Nanotechnology, Monitoring & Management*

Received Date: 18 July 2019

Revised Date: 21 September 2019

Accepted Date: 26 October 2019

Please cite this article as: Grabsi M, Zabat N, Khellaf N, Ismail F, Synthesis of an Environmental Nano-Polyoxometalate ($\alpha_2\text{P}_2\text{W}_{17}\text{CoO}_{61}$)⁸⁻ As Catalyst for Dyes Degradation: A Comparative Study Oxidation of Indigoid And Azo dyes, *Environmental Nanotechnology, Monitoring and amp; Management* (2019), doi: <https://doi.org/10.1016/j.enmm.2019.100269>

This is a PDF file of an article that has undergone enhancements after acceptance, such as the addition of a cover page and metadata, and formatting for readability, but it is not yet the definitive version of record. This version will undergo additional copyediting, typesetting and review before it is published in its final form, but we are providing this version to give early visibility of the article. Please note that, during the production process, errors may be discovered which could affect the content, and all legal disclaimers that apply to the journal pertain.

© 2019 Published by Elsevier.

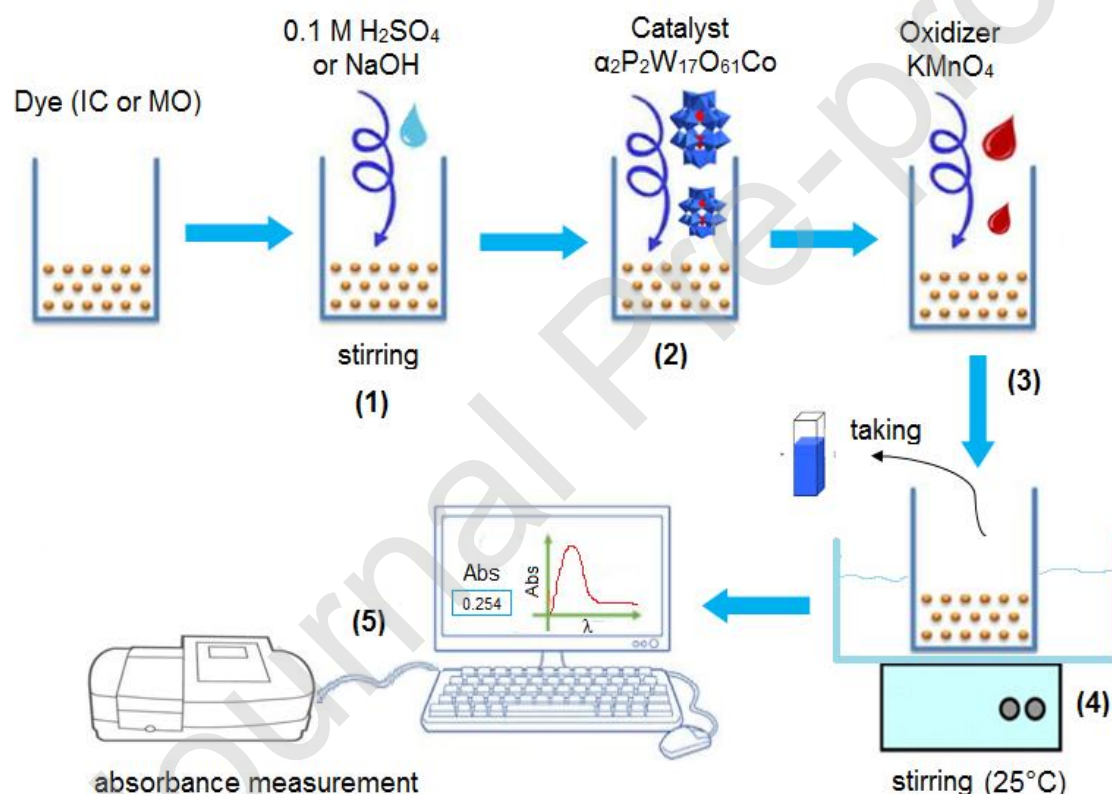
Synthesis of an Environmental Nano-Polyoxometalate ($\alpha_2\text{P}_2\text{W}_{17}\text{CoO}_{61}$)⁸⁻ As Catalyst for Dyes Degradation: A Comparative Study Oxidation of Indigoid And Azo dyes

Mohammed GRABSI¹, Nacéra ZABAT^{1*}, Nabila KHELLAF¹, Fadhe ISMAIL¹

¹Laboratory of Organic Synthesis-Modeling and Optimization of Chemical Processes,
Department of Process Engineering, Faculty of Engineering, Badji Mokhtar-Annaba University, P.O. Box 12
Annaba 23000, Algeria

E-mail: zabatnassira@yahoo.fr

Graphical abstract



Successive steps of procedure for the oxidation of the IC and MO dyes

Highlights

- A cobalt-substituted Wells-Dawson Nano-polyoxometalate ($\alpha_2\text{P}_2\text{W}_{17}\text{O}_{61}\text{Co}$)⁸⁻ was synthesized as catalyst.

- The catalyst prepared was used in the separately oxidation of azoique and indigoid dyes using a new system (dye/ $\text{KMnO}_4/\alpha_2\text{P}_2\text{W}_{17}\text{Co}$).
- The comparative study revealed that the catalytic oxidation of indigo carmine is better than the methyl orange.
- The study of catalyst activity and stability has shown its useful life after four cycles in presence of both dyes separately.
- The analytical methods FT-IR, UV-visible, XRD, FE-SEM and EDX confirmed the stability and robustness of this recovered catalyst after the fourth oxidation cycles.

Abstract

A nanopolyoxometalate (nano-POM) compound consisting of saturated Dawson anions ($\alpha_2\text{P}_2\text{W}_{17}\text{CoO}_{61}$)⁸⁻ has been synthesized and characterized by various analytical methods, UV-Vis spectroscopy, FT-IR spectroscopy, single crystal X-ray Diffraction (XRD), Field Emission Scanning Electron Microscopy (FE-SEM) and Energy Dispersive X-ray analysis (EDX).

The separately oxidative degradation of indigo carmine and methyl orange dyes in aqueous solution by KMnO_4 using ($\alpha_2\text{P}_2\text{W}_{17}\text{CoO}_{61}$)⁸⁻ as catalyst was investigated. The full Decolorization was attained during the first minutes of oxidation process by this new homogeneous system (dye/ $\text{KMnO}_4/\alpha_2\text{P}_2\text{W}_{17}\text{O}_{61}\text{Co}$). The experimental results showed that the catalyst greatly affected the discoloration efficiency; it was up to 75.4% and 66.1% respectively for IC and MO under these optimum conditions: an initial potassium permanganate concentration of 0.02mM, a catalyst concentration of 0.2mM and initial concentration dyes of 5mg/L at pH 3 and room temperature (25°C). The effect of other Dawson type polyoxometalates on the dyes oxidation under the same conditions was evaluated. After four consecutive reaction cycles, the catalyst ($\alpha_2\text{P}_2\text{W}_{17}\text{CoO}_{61}$)⁸⁻ exhibited a good recyclability and reusability without significant loss of activity. The precedents analytical methods indicated that this recovered catalyst has effectively a good stability. This nano-POM function as a recyclable efficient catalyst for the rapid removal of various anionic textile dyes from aqueous solutions.

Keywords: *Polyoxometalate; Nanoparticles; characterization; Degradation; Catalysis; Indigo carmine; methyl orange; KMnO_4*

1. Introduction

Wastewater treatment is one of the major problems facing the chemical, petrochemical, pharmaceutical, and textile industries. These industries generate large quantities of organic pollutants, specially the dyes that cause environmental and health problems [Hassaan and El Nemr 2017]. Azo and indigoid dyes are synthetic organic pigments of great environmental risk due to their toxicity and the potential carcinogenic risk of their degradation products [Ratna and Padhi 2012], combined with their wide usage in textiles, papers, leathers, gasoline, additives, food and cosmetics [Fleischmann et al. 2015]. Thus, it is essential to develop methods to destruct these compounds. In this context, many researchers have studied different techniques such as, biodegradation process [Ramya et al. 2008], advanced oxidation processes [Ortiz et al. 2016], degradation by hypochlorite [Ana de Urzedo et al. 2007], adsorption methods [Crini. 2008], electrochemical oxidation [El-Ashtoukhy. 2013], univariate degradation [Li-Hong et al. 2016], physical methods [Si et al. 2013], biological methods [Parshetti et al. 2007], photochemical and chemical methods [Rezaee et al. 2008] which are the most frequently used for the elimination of indigo carmine and methyl orange from effluent water streams. But, these traditional processes for treatment of the effluents prove to be insufficient to purify wastewater after the different operations of wastewaters dyeing and washing. Over the past decades, significant progress has been achieved in the homogeneous catalysis for the degradation of organics pollutants in aqueous phase, and environmental friendly process to degrade dyes [Bhakya et al. 2015] including nanomaterials, which are an important field of catalysis. Nanomaterials such as TiO_2 [Liu et al. 2018], WO_3 [Alaei et al. 2012], ZnO [Kumar et al. 2014] and polyoxometalates (POMs) [Song and Tsunashima. 2012] have been the primary interest in the pursuit of catalytic materials.

The early transition metals in their highest oxidation state are able to form metal–oxygen cluster anions, commonly referred to as polyoxometalates (POMs) [Long and Cronin. 2012]. The POMs are most well-known as catalysts and have been widely applied in industry [Hill and Kholdeeva. 2013].

The development of highly efficient, easily recovered and reusable based-POM heterogeneous and homogeneous catalysts has long been and will continue to be the focus for the practical application of POMs [Omwomaa et al. 2014; Xiao et al. 2016]. An important property of the Dawson-type Polyoxometalates is the ability to modify the redox and chemical properties of Polyoxometalates by replacing and/or introducing one or more elements, renders them particularly interesting in catalysis. One example of site selective metal substitution was reported in the literatures [Zabat and Abbess. 2015; Zabat. 2018; Zabat. 2019] on the Fe^{2+} , Cu^{2+} and Ni^{2+} substituted of the Wells–Dawson complex

$(\alpha K_6P_2W_{18}O_{62})^{6-}$, through the stereospecific preparation of the lacunary specie $(\alpha_2P_2W_{17}O_{61})^{10-}$. It was successfully used as a catalyst for the oxidation of dyes in aqueous solution.

In this paper the synthesis, characterization and catalytic properties of a new Polyoxometalate complex formed by introducing Co^{2+} ions to the lacunary Polyoxometalate $(\alpha_2P_2W_{17}O_{61})^{10-}$ are reported.

The objective of this work is to investigate the efficiency of potassium permanganate to degrade indigo carmine and methyl orange separately in aqueous solution in presence of $(\alpha_2P_2W_{17}O_{61}Co)^{8-}$ as a catalyst. These dyes are mainly used in the textile industry for dyeing of polyester fibers and denim [Secula et al. 2011]. They have also been used as a food dye, mainly in the juice industry associated with the grape flavor [Yoshioka and Ichihashi. 2008]. The presence of these dyes in residuals cause notorious change of water color and smell even in very low concentration. Moreover, if some of this water reaches natural streams, it can be poisonous for aquatic living entities due to the formation of toxic compounds such as aromatic amines [Campos et al. 2001].

In this work potassium permanganate was chosen because it is a strong oxidizing agent and has several additional advantages over other oxidizing agents: easier handling [Vella and Munder. 1993], an easily soluble solid, and as demonstrated for some contaminants, a higher efficiency of water and soil treatment [Yan and Schwartz. 1999]. It has been applied to the oxidation of certain organic compounds, such as trichlorethylene (TCE) [Yan and Schwartz. 2000], methyl ether of tert-butyl (MTBE) [De Souza Silva et al. 2009], phenanthrene and pyrene [Pandey et al. 2014], isoamyl alcohol and isobutyl alcohol [Massart et al. 1977]. However, up to now no report has been published about the oxidation of indigo carmine and methyl orange dyes by $KMnO_4$ using $\alpha_2P_2W_{17}O_{61}Co$ as catalyst.

The influence of different reactional parameters controlling the separately decolorization of methyl orange and Indigo carmine has been studied.

The activity and the stability of catalyst $(\alpha_2P_2W_{17}O_{61}Co)^{8-}$ after several cycles of oxidation reaction have been also verified.

2. Materials and methods

2.1. Synthesis of Polyoxometalates

The lacunary compound $(\alpha_2K_{10}P_2W_{17}O_{61}, 18H_2O)^{10-}$ in abbreviated $\alpha_2P_2W_{17}$ was prepared from saturated compound $(\alpha K_6P_2W_{18}O_{62}, 20H_2O)^{6-}$ in abbreviated αP_2W_{18} according to the published procedures [Contant and Ciabrini. 1977; Massart et al. 1977]. The compound $\alpha_2P_2W_{17}$ was obtained by the elimination of WO_4^{2-} site from αP_2W_{18} (Fig.1).

The Polyoxometalate used as catalyst ($\alpha_2\text{K}_8\text{P}_2\text{W}_{17}\text{CoO}_{61}, 19\text{H}_2\text{O}$)⁸⁻ in abbreviated $\alpha_2\text{P}_2\text{W}_{17}\text{Co}$ was prepared as the following protocol [Bartis et al. 1999]:

A volume of 10 ml (0.1 M) of $\text{Co}(\text{NO}_3)_3 \cdot 9\text{H}_2\text{O}$ was dissolved in 30 ml of water and 4.7g of $\alpha_2\text{P}_2\text{W}_{17}$ was added with stirring, the product of the reaction was precipitated by adding of 20 ml KCl saturated solution. Finally the crystals that appeared were filtered off and dried in air.

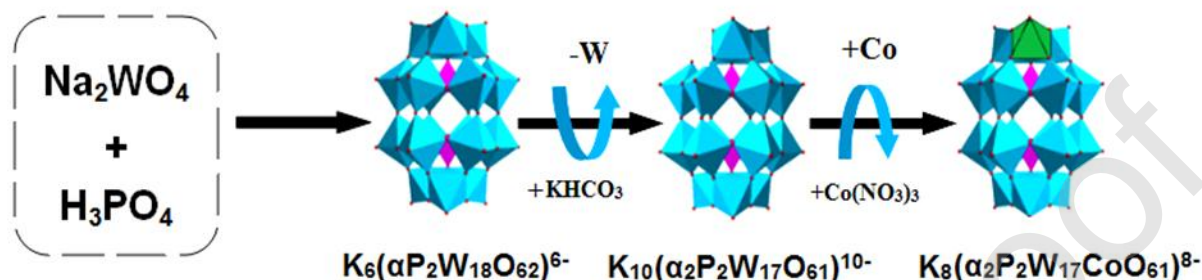


Fig.1. Successive steps of Dawson Polyoxometalates synthesis

2.2. Characterization of Polyoxometalates

The UV-visible spectroscopy measurements were made on a JENWAY 6705 digital spectrophotometer. Quartz vessels with a 10 mm optical path were used.

The set of infrared spectroscopy measurements was recorded by an FT-IR spectrometer K800A-MY14400002. The spectra were processed using the Agilent resolution Pro software.

X-ray diffraction patterns were recorded using a RIGAKU model D/max 2500 diffractometer in the Bragg-Brentano configuration with an anticathode Cu (1.541874 \AA) X-ray tube. The acquisition conditions correspond to an interval of angle 2θ varying from 5 to 90.

The surface morphologies were examined by Field Emission Scanning Electron Microscopy (FE-SEM) using a QUANTA 250 Microscope, equipped with an Energy Dispersive X-ray (EDX) spectroscopy apparatus.

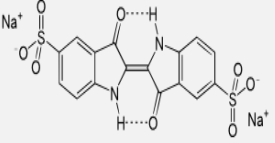
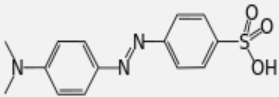
2.3. Oxidation of dyes

2.3.1. Chemicals reagents

Indigo carmine (IC), or cotton blue, acid blue 93, (its molecular formula: $\text{C}_{37}\text{H}_{27}\text{N}_3\text{Na}_2\text{O}_9\text{S}_3$), and Methyl orange (MO) or Acid Orange 52, helianthine B, Orange III, Gold orange, and Tropaeolin D (its molecular formula: $\text{C}_{14}\text{H}_{14}\text{N}_3\text{NaO}_3\text{S}$) were used as model compounds. IC and MO were supplied by Sigma-Aldrich without any purification. Their chemical structures and characteristics are shown in

(Tab.1). The potassium permanganate used in this study was obtained from Merck Chemical Company. All other reagents (NaOH and H₂SO₄) used in this study were analytical grade.

Table 1: Chemical structures and characteristics of IC and MO dyes

Name	Structure	Mw (g.mol ⁻¹)	Chemical class	C.I number	λ_{\max} (nm)
Indigo Carmine E-132		466,353	Indigoid	13015	611
Acid Orange C.I-13025		327,33	Monoazo	13025	506

2.3.2. Procedure for the oxidation of the IC and MO

The oxidation of the IC and MO was realized separately in batch reactor of 200ml capacity at room temperature. To 100 ml of dyes solutions (MO) and (IC) at initial concentrations of 10 mg/L, an appropriate amount of catalyst ($\alpha_2\text{P}_2\text{W}_{17}\text{Co}$) was added. For all experiments the initial concentration of dye was kept constant except for those carried out to examine the effect of initial dye concentration. The pH of the reaction was adjusted with (0.1M) H₂SO₄ or (0.1M) NaOH in aqueous solutions using HANNA pH meter. A magnetic stirrer was used to ensure uniform mixing of aqueous solution. Then a volume of the oxidant (KMnO₄) at a known concentration was added. At this time, the oxidation reaction was initiated. At regular time intervals (2min) for the reaction with IC or MO, 2 mL of the sample was collected from the reactor for measurements of dyes absorbance using a 6705 UV-Visible spectrophotometer JENWAY.

The wavelength corresponding to the maximum absorbance of (IC) is (λ_{\max} = 611 nm) [Secula et al. 2011], considering that this dye is very stable in aqueous medium. However, for the MO its color varies according to the medium pH. For this reason, the absorbance of MO solution was registered versus medium pH in the range of [400 - 800nm] [Zabat. 2019], to determine the maximum wavelength (λ_{\max}) of the MO.

The oxidation of dyes was performed according to the following factors: initial pH of solution, oxidant concentration, catalyst concentration, initial dye concentration. The effect of temperature and type of POMs were also studied.

The decolorization efficiency (%) of dyes has been calculated as:

$$DE = \left[\frac{(Ci - Cf)}{Ci} \right] \times 100$$

Where: DE (%) is the decolorization efficiency; C_i (mg/L) is the initial concentration of dyes and C_f (mg/L) is the final concentration of dyes.

3. Results and discussion

3.1. Characterization of Polyoxometalates

3.1.1. UV-Visible spectroscopy

The UV-Vis spectroscopy allowed us to characterize the three polyoxometalates synthesized through the main absorption bands observed on (Fig.2).

The UV-visible spectra exhibit intense absorption bands between 200 and 300 nm with maxima wavelengths which are 218, 211 and 220 nm for polyoxometalates P_2W_{18} , P_2W_{17} and $P_2W_{17}Co$ respectively, these bands correspond to an electronic transition π -d of the band ($O_d \rightarrow M$) [Li et al. 2013].

The wide bands observed at around 270 nm are assigned to the π -d electronic transitions of the band ($O_b / O_c \rightarrow M$) ($M = W, Co$) [Li et al. 2013]. Thus, the mono-substituted compound $P_2W_{17}Co$ and the parent compound P_2W_{18} have similar characteristics, only the main peak of $P_2W_{17}Co$ shifts slightly towards the visible (217 nm at 220 nm), but there is no visible absorbance.

Prior determination of the absorption range of catalyst $P_2W_{17}Co$ is necessary in this study, to avoid the problem of interference between the wavelengths of the latter and the dyes used. It is deduced that the $P_2W_{17}Co$ catalyst absorbs in the UV range, with a maximum length of 220 nm. As indigo carmine and methyl orange absorb in the visible, and $P_2W_{17}Co$ catalyst does not absorb substantially in this area, any risk of interference is therefore excluded.

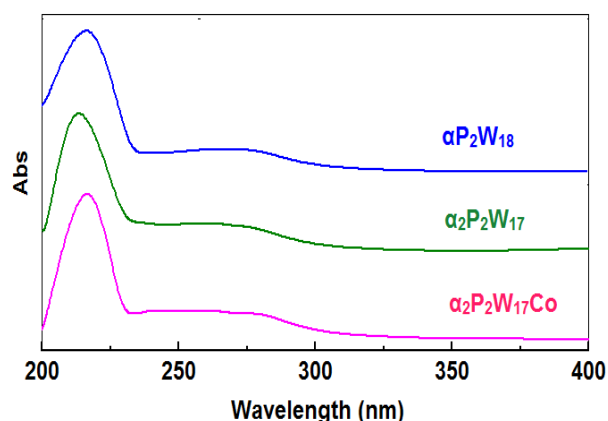


Fig.2. UV-Vis spectrums of synthesized Polyoxometalates

3.1.2.FT-IR Spectroscopy

(Fig.3) represents the IR spectra for the three polyoxometalates P_2W_{18} , P_2W_{17} and $P_2W_{17}Co$.

The IR spectrum of monolacunaire P_2W_{17} compound, noticed the presence of an additional P-O band located at 1046 cm^{-1} , the existence of this band corresponds to a significant disruption in a direction of the PO_4 tetrahedron [Rocchiccioli-Deltcheff and Thouvenot, 1979]. This band disappears for the monosubstituted compound $P_2W_{17}Co$ after the addition of the Co^{2+} ion to P_2W_{17} lacunar compound. Finally, it is obtained a spectrum similar to that of P_2W_{18} . This shows the possibility of creating lacunar compounds that tend to fill their gap with substitution elements, in order to form new saturated substituted (POM)s.

The bands at about 3531 cm^{-1} and 1612 cm^{-1} were assigned to the stretching vibration of O-H bonds and the bending vibration of H-O-H bonds, respectively. Generally (Table.2) resumes all the characteristic bands of the Dawson structure which appear on the spectra of the three (POM)s [Contant et al. 1997] in the $700\text{-}1100\text{ cm}^{-1}$ region. The vibration frequencies are in descending order according to: $\text{vas}(P-Oa) > \text{vas}(M-Od) > \text{vas}(M-Ob-M) > \text{vas}(M-Oc-M)$, ($M = W, Co$).

Table 2: IR vibration frequencies of synthesized polyoxometalates

Compound	$\text{vas}(P-Oa)$	$\text{vas}(M-Od)$	$\text{vas}(M-Ob-M)$	$\text{vas}(M-Oc-M)$
αP_2W_{18}	1086	952	900	718
$\alpha_2 P_2W_{17}$	1077	937	880	704
$\alpha_2 P_2W_{17}Co$	1079	956	908	751

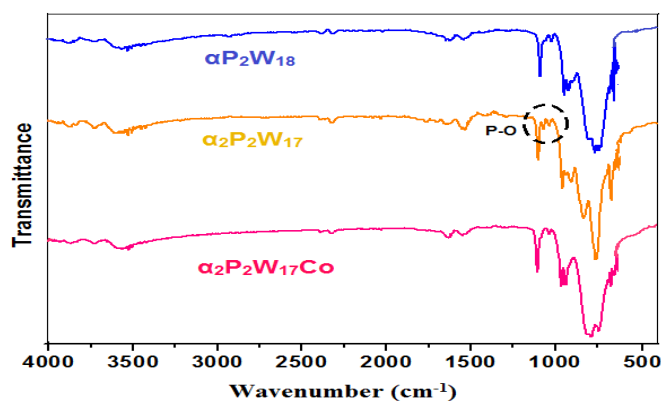


Fig.3. Infra-red spectra of synthesized Polyoxometalates

3.1.3. X-Ray Diffraction

X-ray diffraction is a good way to identify the structure of POMs. The DRX diffractograms of the three (POM)s are shown in (Fig.4). According to this figure, the main diffraction angles 2θ are observed at (7.1° , 8.0° , 9.3° , 12.8° , 15.0° , 18.1° , 24.7° , 24.9° , 25.5° , 26.6° , 28.8°); (6.5° , 8.2° , 9.1° , 13.7° , 14.2° , 18.2° , 24.3° , 24.5° , 25.2° , 27.6° , 29.8°) and (7.6° , 8.1° , 8.9° , 12.7° , 14.7° , 17.9° , 24.0° , 24.9° , 25.1° , 27.5° , 29.3°) for the POMs $\alpha\text{P}_2\text{W}_{18}$, $\alpha_2\text{P}_2\text{W}_{17}$ and $\alpha_2\text{P}_2\text{W}_{17}\text{Co}$ respectively. These results are similar to those reported in the literatures [Briand et al. 2002, Qian et al. 2011], which show characteristic peaks of Dawson structure. Also, the intense signals observed at $2\theta < 10^\circ$ indicate that the three POMs contain only α -isomer of the Dawson structure [Pope. 2001].

The other peaks appearing on the diffractograms of the three POMs represent the residues of the synthesis. For lacunary polyoxometalate $\alpha_2\text{P}_2\text{W}_{17}$, the peaks appear a little bit larger than those of $\alpha\text{P}_2\text{W}_{18}$ because of the elimination of the tungstic group WO_4^{2-} , but it still keeps the peaks characterizing the Dawson structure, this small change was disappeared after filling the gap by the substitution of the metallic cation Co^{2+} for the lacunar species $\alpha_2\text{P}_2\text{W}_{17}$. Finally, the substituted $\alpha_2\text{P}_2\text{W}_{17}\text{Co}$ polyoxometalate is obtained, which has a diffractogram similar to that of $\alpha\text{P}_2\text{W}_{18}$ compound. This observation is in agreement with the FT-IR analysis, which also shows the filling of gap by the Co^{2+} cation.

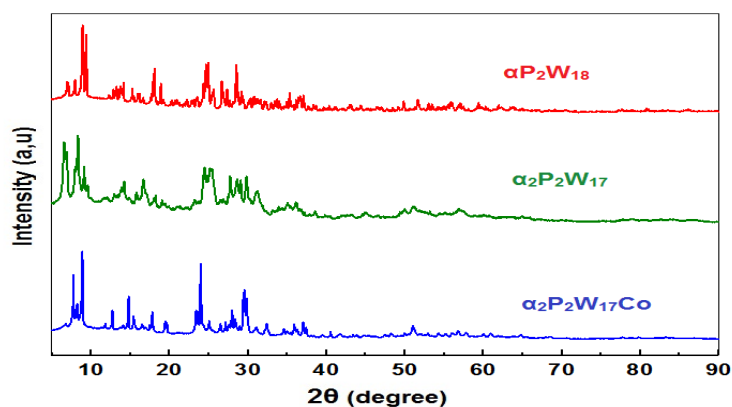


Fig.4. X-Ray diffraction of synthesized Polyoxometalates in powder form

3.1.4. FE-SEM and EDX analysis

The morphological properties and microstructure of the three polyoxometalates were clarified by observations of SEM scanning electron microscopy. The SEM images are indicated on (Fig5).

The SEM images show that the nanoparticles of the parent polyoxometalate P_2W_{18} (Fig.5a) and lacunary P_2W_{17} (Fig.5b) are distinguished by an irregular polyhedric aggregate, but without noticing a change in microstructure and morphology of P_2W_{17} nanoparticles after removal of WO_4^{2-} tungstic group. For the monosubstituted polyoxometalate $P_2W_{17}Co$ (Fig.5.c), and after the incorporation of the metal cation Co^{2+} , a change is observed on the microstructure and the morphology of the nanoparticles, and that the majority of the nanoparticles gives an aggregate which has a shape similar to the cubic form. The heterogeneous shape and size of the monosubstituted polyoxometalates $P_2W_{17}Co$ nanoparticles gives a high porosity appeared by a large number of cavities, which logically increases the specific surface area of this catalyst [Jarrah and Farhadi. 2019]. Therefore, it is suggested that the porous surface of $P_2W_{17}Co$ gives an important characteristic to increase efficiency and catalytic activity.

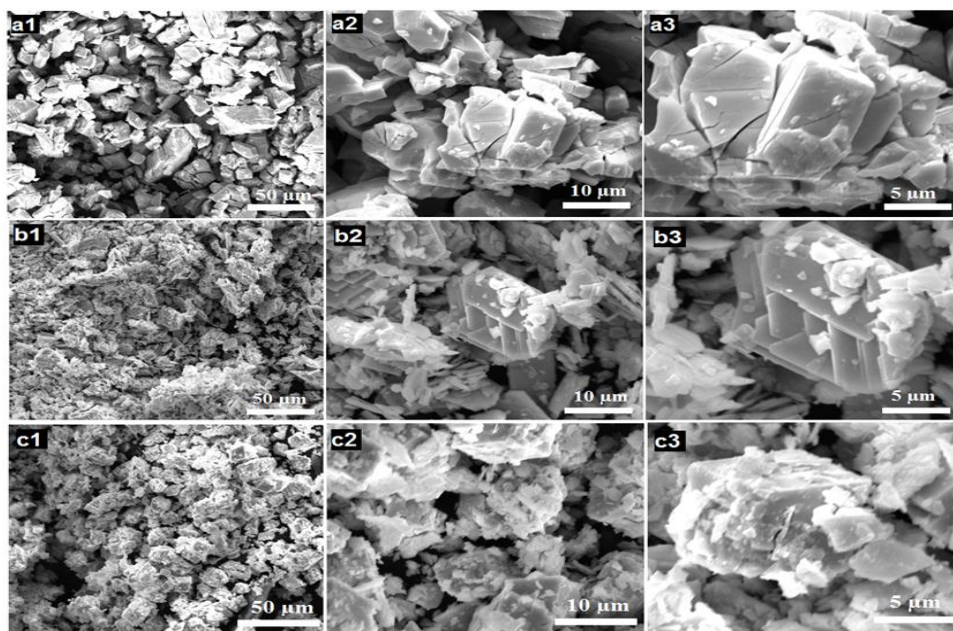


Fig.5. FE-SEM photographs of P_2W_{18} (a), P_2W_{17} (b) and $P_2W_{17}Co$ (c) at different magnifications

The (Fig.6) represents the EDX spectrogram of the elemental analysis of the three polyoxometalates. The presence of the peaks that correspond to the elements P, O, K and W have been proven in the chemical composition of P_2W_{18} and P_2W_{17} .

For the monosubstituted polyoxometalate $P_2W_{17}Co$, the appearance of the new peaks corresponding to cobalt (Co) was observed, this appearance is logically due to the substitution of the metallic element Co^{2+} for the monolacunary compound P_2W_{17} . It can be seen that the chemical elements appearing on the EDX spectrogram are uniformly distributed over these three polyoxometallates, confirming the homogeneity of the samples studied. Thus, the $P_2W_{17}Co$ EDX spectrogram confirms the uniform incorporation of the cobalt Co^{2+} element into the P_2W_{17} monolacunary compound. It is clear that the proportions of tungsten W and oxygen O are the highest for the three synthesized POMs, which corresponds absolutely to the polyoxometalates of Dawson structure.

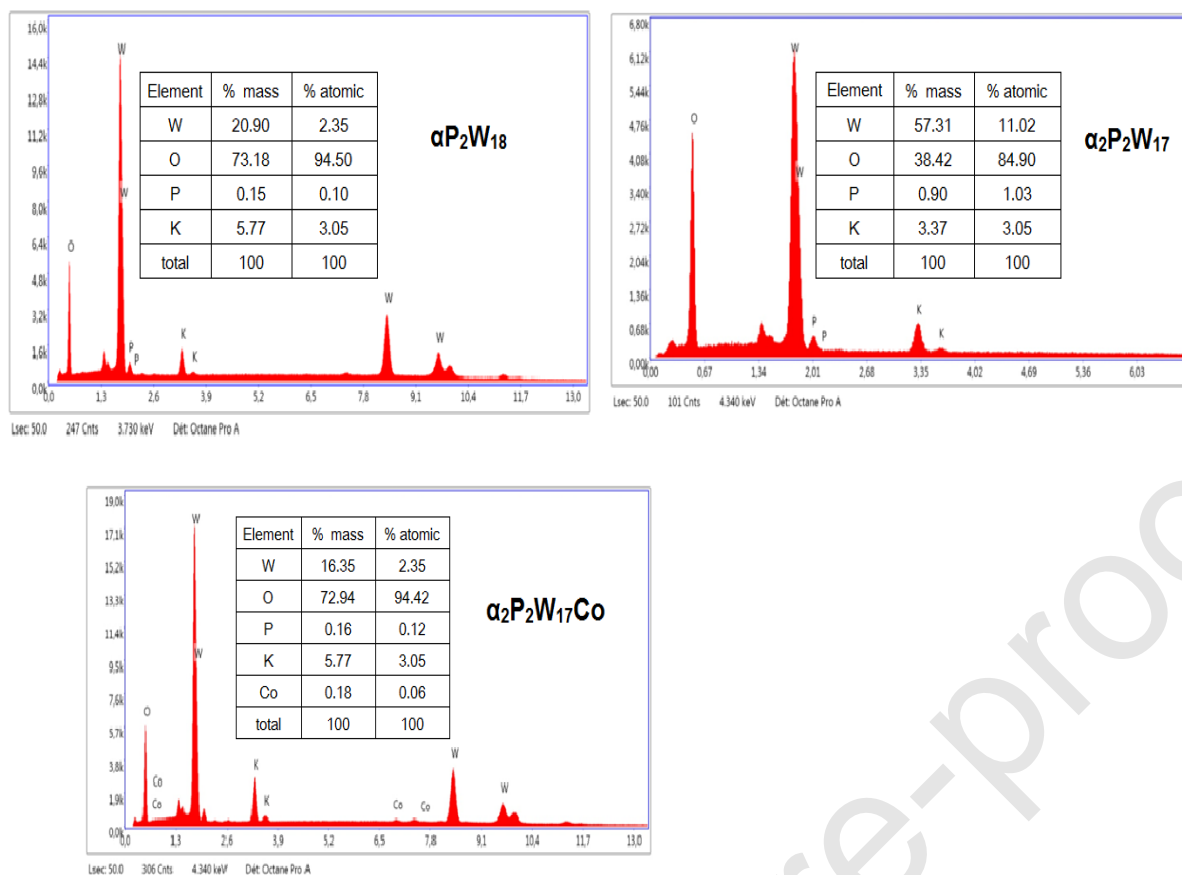


Fig.6. EDX spectra of synthesized Polyoxometalates in powder form

The combination of the DRX and SEM-EDX results with the previous analysis of FT-IR and UV-Vis confirms that the POMs $\alpha\text{P}_2\text{W}_{18}$, $\alpha_2\text{P}_2\text{W}_{17}$ and $\alpha_2\text{P}_2\text{W}_{17}\text{Co}$ have a Dawson structure.

3.2. Oxidation of dyes

3.2.1. Effect of operating conditions on the degradation of IC and MO dyes

Generally, the catalytic activity of a catalyst is influenced by the reaction parameters. Thus, to achieve the best decolorization yield of indigo carmine and methyl orange, the optimization of experimental oxidation conditions was studied. Different parameters were examined.

3.2.1.1. Effect of initial pH

In permanganate oxidation, pH is considered important because it strongly influences the redox potential in a given system [Aleboyeh et al. 2009]. To highlight the pH influence on the stability of catalyst used ($\text{P}_2\text{W}_{17}\text{Co}$) in the degradation of IC and MO by KMnO_4 , the pH was ranged between 3 and 10.

In this work the more acidic pH was avoided, in order to prevent the risk of dimerization of the catalyst; while for pH greater than 10, the catalyst is likely to degrade [Pope. 1983].

According to the results obtained in (Fig.7), the oxidation by KMnO_4 is strongly influenced by the pH of the reaction medium, the maximum discolorations of IC and MO are respectively (27.2%) and (29.4%) at acidic pH (pH=3). Then, the discoloration efficiency is reduced gradually moving to natural and basic media. These results are similar to those got by Xiang-Rong Xu et al. [Xiang-Rong et al. 2005] Aleboyeh et al [Aleboyeh et al. 2009], Azmat et al [Azmat et al. 2011], they reported that the oxidation potential (E°) increases with decreasing pH for dyes, and the (E°) in acidic solution is much higher than in alkaline and neutral solution. That is explained by the potassium permanganate behavior, because in acidic condition, KMnO_4 exhibits high oxidative reactivity with oxidation potential (E°) of +1.51 V, and its reductive product is Mn^{2+} [Eq. (1)]. However, KMnO_4 shows (E°) value of +0.59 V in neutral and alkaline conditions which results of hydrous manganese dioxide (MnO_2) formation [Eq. (2)]. So, more the solution is acidic, greater the oxidation ability of potassium permanganate. In addition, the fall of discoloration efficiency in natural and basic media can be related to the catalyst stability interval used, because the majority of (POM)s Dawson type are only stable in acidic media [Schwegler. 1991].

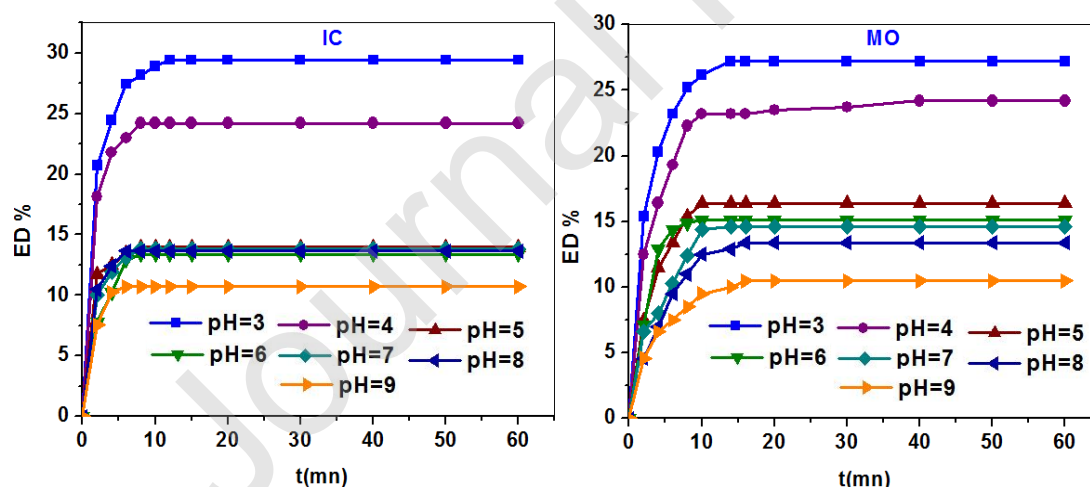
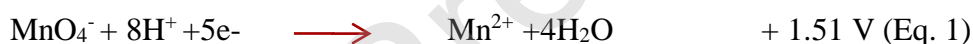


Fig.7. Effect of initial pH on the decolorization of IC and MO during oxidation catalyzed by $\text{P}_2\text{W}_{17}\text{Co}$ (Conditions: $V_R=100 \text{ mL}$, $[\text{Dye}]_0=10\text{mg/L}$, $[\text{Cat}]=0.2 \text{ mM}$, $T=25^\circ\text{C}$, $[\text{KMnO}_4]=0.01\text{mM}$).

3.2.1.2. Effect of potassium permanganate concentration

The study of the oxidant concentration effect on the catalytic oxidation reaction of IC and MO was verified by varying the initial KMnO_4 concentration from 0.005 to 0.2 mM.

According to the results shown in (Fig.8), the color removal of the two dyes increased with the increasing concentration of potassium permanganate. These results display that the decolorization efficiencies of IC and MO obtained are 97.01% and 85.1% respectively, at a potassium permanganate concentration of 0.2 mM. This proves a strong reactivity of these two dyes with KMnO_4 . Also, these results are explained by the increase of KMnO_4 concentration, where more permanganate ions (MnO_4^-) are available to oxidize the molecules of the two dyes [Razi Khan et al. 2016]. Therefore, the increase of the quantity of molecules of oxidant per unit of volume, leads to the destruction of the functional groups $\text{C}=\text{C}$ and $\text{N}=\text{N}$, as well as to the opening of the aromatic rings, due to the rupture of the double bonds $\text{C}=\text{C}$ cycles, this logically increases the probability of the collision between organic molecules and the oxidation species, leading to an increase in fading efficiency [Damm et al. 2002]. On the other hand, large concentrations of KMnO_4 should be avoided because they can induce excess ions (Mn^{2+}) that are formed in acidic medium (see eq1); thus leading to a toxic effect by the inhibition of the catalyst ($\text{P}_2\text{W}_{17}\text{Co}$) [Inam et al. 2016].

As the oxidation potential of KMnO_4 is very strong, therefore the high concentrations of the latter must be avoided, and this to highlight the effect of the catalyst ($\text{P}_2\text{W}_{17}\text{Co}$) on the oxidation efficiency. For this, an average concentration of KMnO_4 equal to 0.02 Mm was chosen, in order to continue the comparative oxidation study of IC and MO.

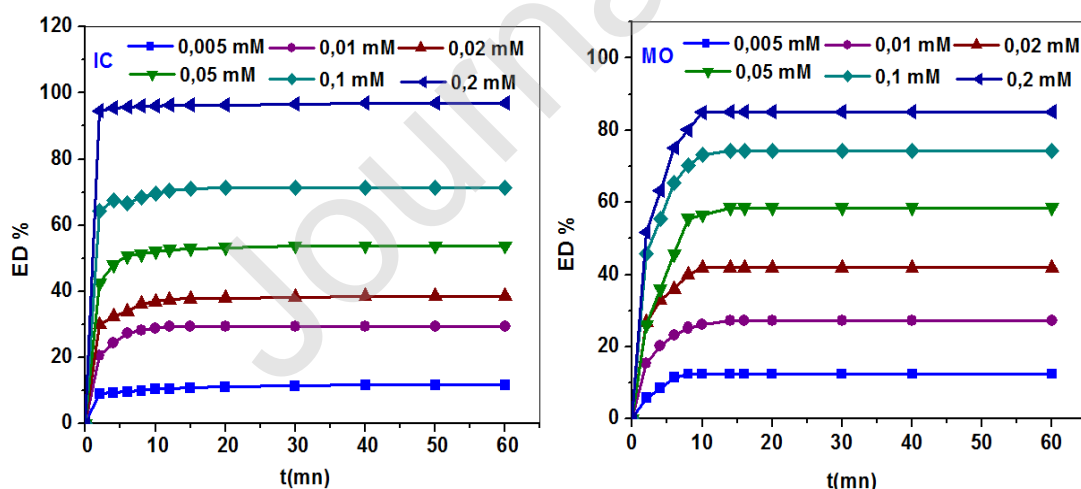


Fig.8. Effect of initial concentration KMnO_4 on the decolorization of IC and MO during oxidation catalyzed by $\text{P}_2\text{W}_{17}\text{Co}$ (Conditions: $V_R=100$ mL, $\text{pH}=3$, $[\text{Dye}]_0=10$ mg/L, $[\text{Cat}]=0.2\text{mM}$, $T=25^\circ\text{C}$)

3.2.1.3. Effect of catalyst concentration

The optimal concentration of the catalyst is an important parameter to study to avoid the excess which could make the process less profitable.

The study of the catalytic oxidation efficiency of IC and MO is carried out at different concentrations of the catalyst ($P_2W_{17}Co$) ranging from 0.1mM to 0.7mM, for a dye concentration of 10 mg/L at the previous optimum parameters (pH =3 and C_{KMnO_4} = 0.02 Mm). The results of discoloration are shown in (Fig.9).

According to (Fig.9), the catalyst concentration has a significant effect on the decolorization efficiency of MO and IC in the presence of $KMnO_4$. From where, without catalyst (ED=7.8%) for IC and (ED=8.58%) for MO. However, after the addition of catalyst ($P_2W_{17}Co$) the efficiency of decolorization improves, and it becomes directly proportional to the concentration of the catalyst until a concentration equal to 0, 2mM for IC (ED =41.3%), and 0.3mM for MO (ED =50.1%). This positive effect on the oxidation reaction is explained by the presence of $P_2W_{17}Co$ as catalyst, but it is noted that beyond these concentrations, the decolorization efficiency remains stable, where the overdose of the catalyst is not useful. These results are observed in the literatures [Troupis et al. 2007; Wang and Yang. 2010] using the system (dye/oxidant / POM) which show that the addition of the catalyst proportionally increases the decolorization efficiency, but for an excess of concentration, the decolorization efficiency remains constant due to the saturation of the catalyst. This evidences that an excessive increase of the catalyst concentration in the presence of a sufficiently strong oxidant such as $KMnO_4$ becomes insignificant, because at 0.2mM and 0.3mM of the catalyst ($P_2W_{17}Co$), the decolorization efficiency for IC and MO reaches almost its maximum [Bu et al. 2017]. As, an excess catalyst concentration is not important, the maximum loss of the catalyst, must be reduced for purely economic reasons. So, the optimal concentration of ($P_2W_{17}Co$) chosen is 0.2 mM to complete the comparative study.

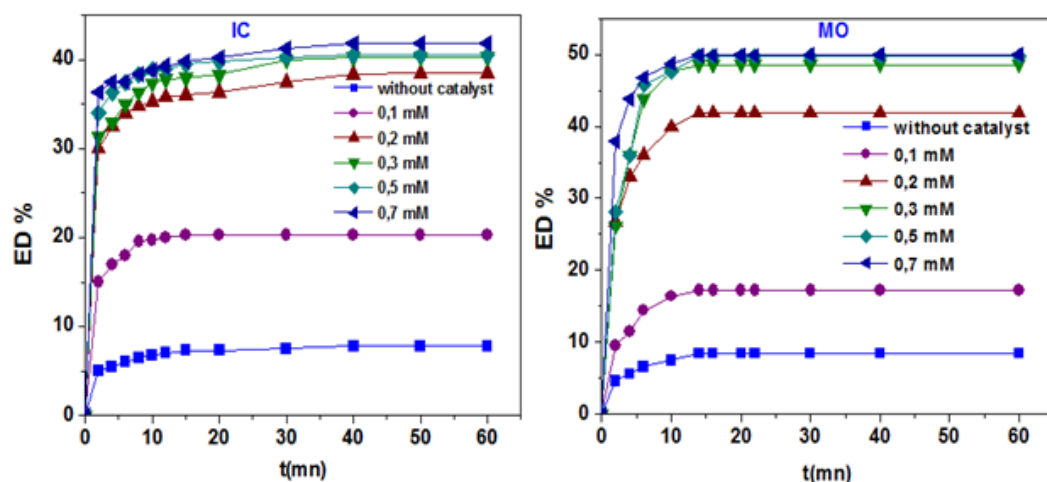


Fig.9.Effect of catalyst concentration on the decolorization of IC and MO during oxidation catalyzed by $P_2W_{17}Co$ (Conditions: $V_R=100$ mL, $pH=3$, $[Dye]_0=10$ mg/L, $[KMnO_4]=0.02$ mM, $T=25^\circ C$)

3.2.1.4. Effect of initial concentration of IC and MO dyes

In wastewater treatment, the concentration of the organic pollutant is a very important parameter. For this reason, the influence of the initial concentration of IC and MO on the $KMnO_4$ decolorization process in the presence of catalyst ($P_2W_{17}Co$) was studied. The initial concentrations of IC and MO were ranged between 5 and 25 mg/L, keeping the same operating conditions mentioned above. The results obtained are illustrated on (Fig.10).

On (Fig.10) it is observed that the decolorization efficiency decreases with the increase of the initial concentration of the two dyes. These results agree with what has been stated in several literatures [Devi et al. 2007; Abou-Gamra. 2014; Reza et al. 2016], which explained this observed decrease in efficiency when increasing the concentration of dye, by a logical increase in dye molecules which inevitably leads to a limiting step because of the lack of MnO_4^- ions to oxidize all the molecules of the dye. This increase in dye also reduces the catalytic activity because of the coverage of the active sites of the $P_2W_{17}Co$ catalyst by the molecules of the accumulated dyes.

In other research [Neppolian et al. 2002], it is concluded that as the initial dye concentration increases, the requirement for the amount of catalyst needed for the degradation to increase as well. Therefore, their optimization is necessary. The best discoloration efficiencies respectively for IC and MO are (ED=75.4%) and (ED=66.1%) for an optimal concentration of the two dyes equal to 5 mg/L.

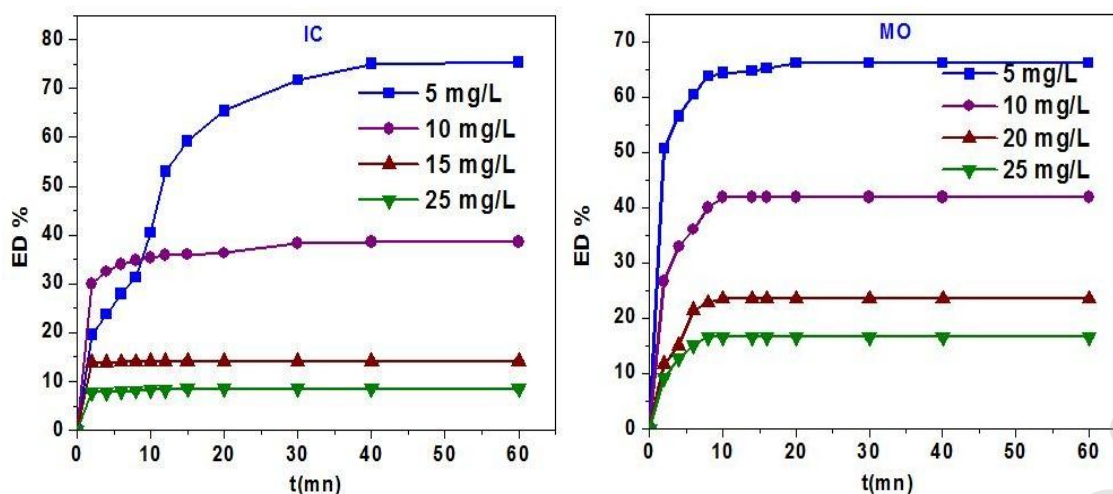


Fig.10. Effect of initial concentration dye on the Decolorization of IC and MO during oxidation catalysed by $P_2W_{17}Co$ (Conditions: $V_R=100$ mL, $pH=3$, $[Cat]=0.2mM$, $[KMnO_4]=0.02mM$, $T=25^\circ C$)

3.2.1.5. Effect of temperature

Temperature is an important kinetic factor. It can have a great influence on the performance of the oxidant; as well as the activity and stability of the catalyst that can be modified by a different reaction temperature. From where, the effect of temperature on the discoloration of IC and MO solutions was carried out at a temperature range of $25^\circ C$ to $60^\circ C$.

According to (Fig.11), it is noticed that the increase of the temperature from $25^\circ C$ to $60^\circ C$ does not have a significant effect on the discoloration efficiency of the two dyes, which passes from 75.4% at 79.2% for indigo carmine, and from 66.1% to 70.2% for methyl orange. This observation has been noted by several authors [Aleboyeh et al. 2009; Xiang-Rong et al. 2005; Olya et al. 2012] who confirm that temperature is not an important parameter in potassium permanganate oxidation processes. Since the effect of the temperature increase was not significant for the both dyes, because 75% of the decolorization efficiency can be obtained at room temperature ($25^\circ C$). So, the choice of room temperature ($25^\circ C$) allows us to reduce operational capital costs in the actual wastewater treatment processes.

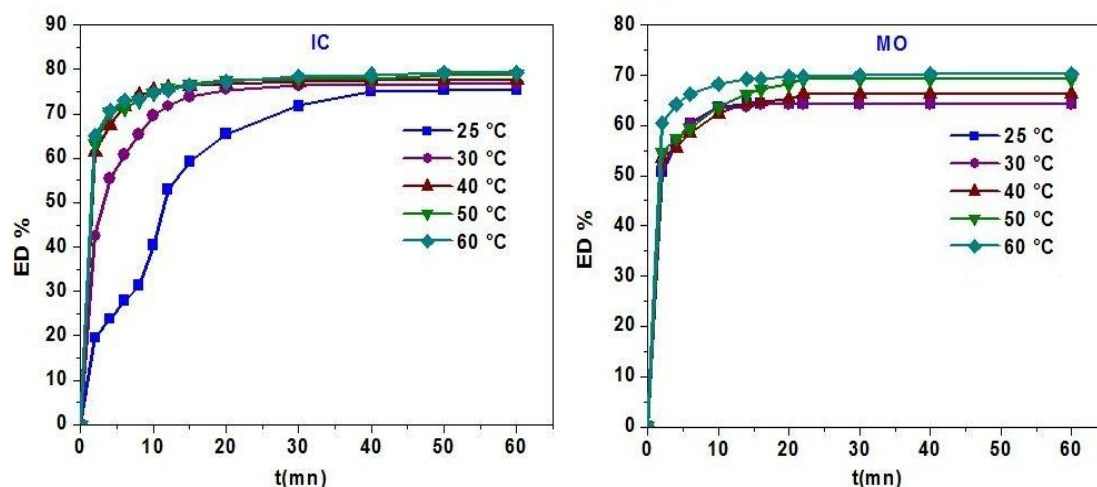


Fig.11. Effect of temperature on the decolorization of IC and MO during oxidation catalyzed by $P_2W_{17}Co$ (Conditions: $V_R=100$ mL, $pH=3$, $[Dye]=5mg/L$, $[Cat]=0.2mM$, $[KMnO_4]=0.02mM$)

3.2.1.6.UV- Vis absorbance spectra of dye before and after oxidation

According to the UV-Vis spectra shown in (Fig.12), the degradation of IC and MO by the system ($KMnO_4/P_2W_{17}O_{61}Co$) is confirmed.

From a kinetic point of view, the catalytic oxidation by $KMnO_4$ of the two dyes occurs in two stages: a very fast first and a slow second. We can note that more than 70% of the degradation was done in the first step where the majority of the introduced $KMnO_4$ was consumed. Beyond this step it was noticed that the variation of consumption in $KMnO_4$ becomes more or less weak, the oxidation rate becomes slower and stops completely after a period of 60 minutes of contact.

The degradation was followed by recording a progressive reduction of the indigo absorption band of IC at 611 nm and the azo band of MO at 506 nm, these bands correspond to the functional groups $C=C$ and $N=N$ of indigo carmine and methyl orange respectively. These bands are the source of dye hue, and are very sensitive to oxidation by the MnO_4^- agent. This observation is consistent with the literatures [Azmat et al. 2007; Zabat. 2019], which confirm that $KMnO_4$ has the property of easily oxidizing $C=C$ and $N=N$ double bands in indigo and azo compounds, noting its strong oxidation potential with respect to these dyes.

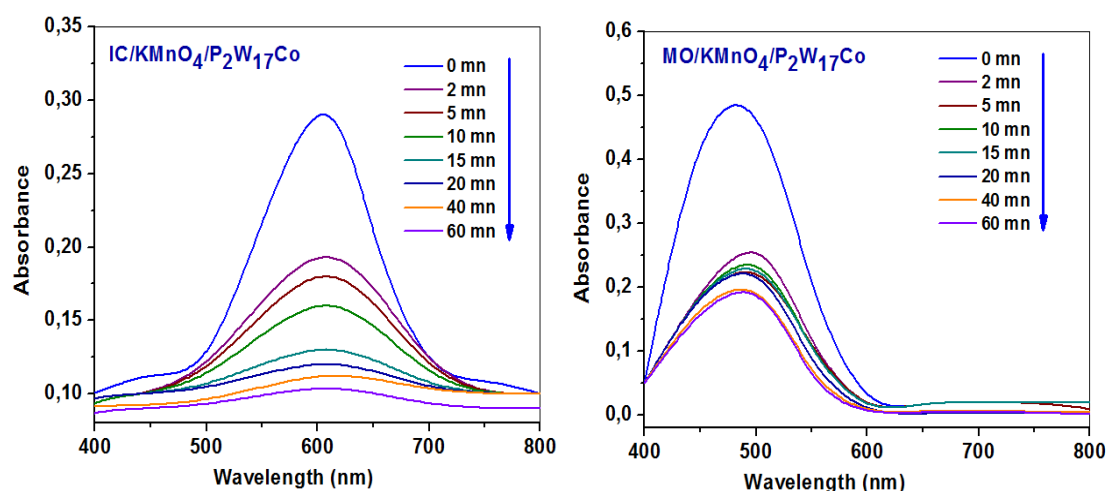


Fig.12. UV-vis spectra of Indigo carmine and Methyl Orange before and after 1h of catalytic oxidation. (Conditions: $V_R=100\text{mL}$, $\text{pH}=3$, $[\text{Dye}]=5\text{mg/L}$, $[\text{Cat}]=0.2\text{mM}$, $[\text{KMnO}_4]=0.02\text{mM}$, $T=25^\circ\text{C}$)

3.2.1.7. Effect of catalyst nature

At the end of this study, the performance of this substituted $\text{P}_2\text{W}_{17}\text{Co}$ catalyst with parent compound P_2W_{18} and other substituted Polyoxometalates of Dawson structure X-POM ($X = \text{Co}^{2+}$, Cu^{2+} , Ni^{2+} , Mo^{2+}) was compared.

The results exposed in (Fig.13) show that the discoloration efficiency of the two dyes IC and MO varies significantly with the nature of the tested catalyst. Hence, for indigo carmine: $\{\text{ED}(\text{P}_2\text{W}_{17}\text{Co}) = 75.4\%\}$; $\{\text{ED}(\text{P}_2\text{W}_{18}) = 29.3\%\}$; $\{\text{ED}(\text{P}_2\text{W}_{17}\text{Cu}) = 37.2\%\}$; $\{\text{ED}(\text{P}_2\text{W}_{17}\text{Ni}) = 40.9\%\}$; $\{\text{ED}(\text{P}_2\text{W}_{15}\text{Mo}_2\text{Co}) = 49.1\%\}$. By cons for methyl orange: $\{\text{ED}(\text{P}_2\text{W}_{17}\text{Co}) = 66.1\%\}$; $\{\text{ED}(\text{P}_2\text{W}_{18}) = 31.2\%\}$; $\{\text{ED}(\text{P}_2\text{W}_{17}\text{Cu}) = 58.5\%\}$; $\{\text{ED}(\text{P}_2\text{W}_{17}\text{Ni}) = 60.4\%\}$; $\{\text{ED}(\text{P}_2\text{W}_{15}\text{Mo}_2\text{Co}) = 45.8\%\}$.

These results show that substitution of the transition metal by cations such as Co^{2+} , Cu^{2+} , Ni^{2+} , and Mo^{2+} on the incomplete polytungstic matrix can effectively enhance the catalytic activity of saturated and lacunars (POM)s across the W-O-W band [Shojaei et al. 2011; Troupis et al. 2009] .

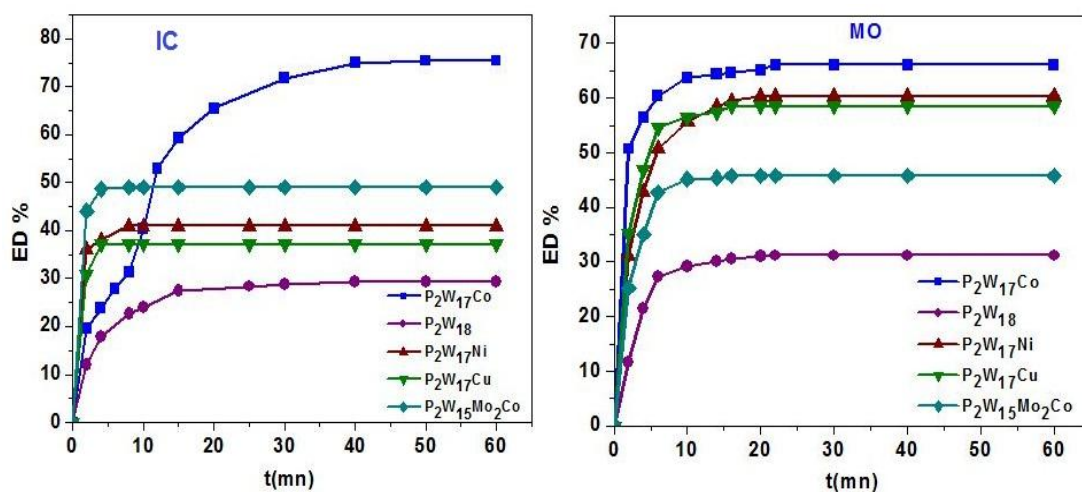


Fig.13.Effect of the catalyst nature on the degradation of IC and MO during oxidation catalyzed by X-POM (Conditions: $V_R=100$ mL, $pH=3$, $[Dye]=5$ mg/L, $[Cat]=0.2$ mM, $[KMnO_4]=0.02$ mM, $T=25^\circ C$)

3.3. Activity and stability of the catalyst ($P_2W_{17}Co$)

In order to verify the stability and the catalytic performance of the $P_2W_{17}Co$, at the end of the oxidations reactions, the catalyst was reused at four cycles in the same initial solution (without recovering it), each time adjusting the initial concentration of the dye to the end of each cycle. The oxidations reactions of MO and IC with $KMnO_4$ in the presence of $P_2W_{17}Co$ catalyst were carried out under the same previous operating conditions.

(Fig. 14) shows a gradual drop in discoloration efficiency from 75.4% to 60.8% at the end of the fourth cycle for indigo carmine and from 66.1% to 46.7% for methyl orange. This result can be explained by the formation of an excess of the Mn^{2+} colloidal particles which can be superimposed on the catalyst surface [Doré. 1989], thus leading to the decrease of the catalytic activity of the catalyst $P_2W_{17}Co$. This decrease can also be due to the accumulation of dye molecules on the catalyst surface, because the latter has not been regenerated, which leads to the saturation of its surface and therefore to its deactivation [Mahmoodi et al. 2011].

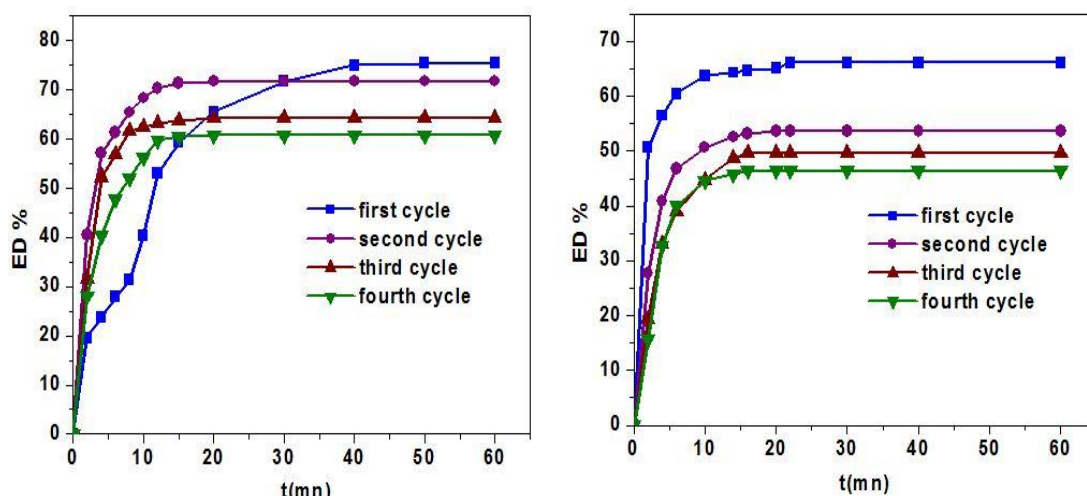


Fig.14. Catalytic performance of catalyst for four cycles through the oxidation of IC dye catalyzed by $P_2W_{17}Co$ (Conditions: $V_R=100$ mL, $pH=3$, $[Dye]=5$ mg/L, $[Cat]=0.2$ mM, $[KMnO_4]=0.02$ mM, $T=25^\circ C$)

For the catalyst resumes its maximum profitability at the end of the chemical reaction, it is sufficient that it be recovered and washed to remove impurities suspended on its surface. For this, after the four cycles of $P_2W_{17}Co$ use, the latter was recovered by gradually adding a mass of KCl to the colored solution until the formation of a precipitate, and the catalyst was separated by a simple filtration.

In order to verify the stability of recovered $P_2W_{17}Co$, it was dried at room temperature ($25^\circ C$) to remove all water or organic molecules, and was characterized by spectroscopic techniques such as: UV-vis, FT-IR, DRX and MEB-EDX.

3.4. Characterization of recovered $P_2W_{17}Co$

3.4.1. UV-Visible spectroscopy

It is observed that after the four oxidation cycles, the two recovered Polyoxometalates spectra shown in (Fig.15) are identical to the initial spectra catalyst, they constantly represent two main peaks at around 220 and 270 nm [Li et al. 2013], always corresponding to an electronic transition $\pi-d$ of the bands ($Od \rightarrow M$) and ($Ob / Oc \rightarrow M$) respectively.

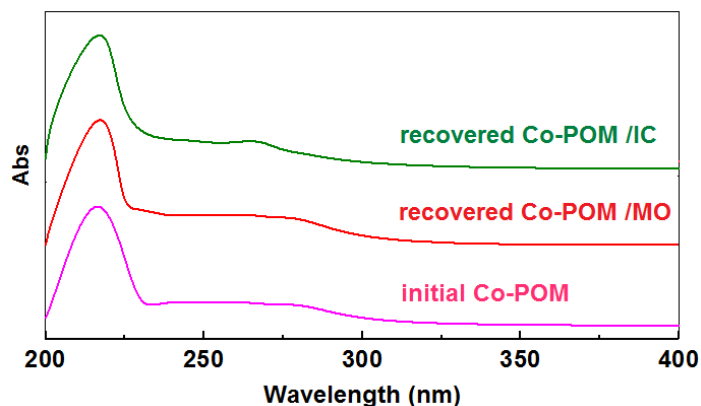


Fig.15. UV-vis spectra of recovered $P_2W_{17}Co$ (POM) after four cycle of oxidation

3.4.2.FT-IR Spectroscopy

(Fig.16) represents the IR spectra of recovered $P_2W_{17}Co$ after the four oxidation cycles of the two dyes. The set of vibration bands are grouped in the (Tab.3)

Generally (Tab3) shows that all the characteristic bands of the Dawson structure, appear on the spectra of the recovered catalyst which are always in the $700-1100\text{ cm}^{-1}$ region.

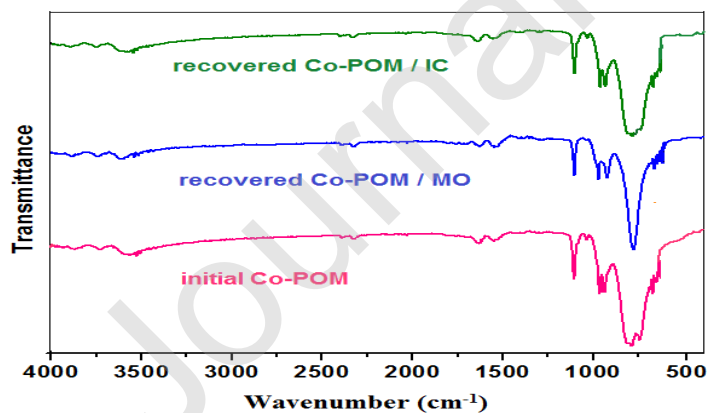


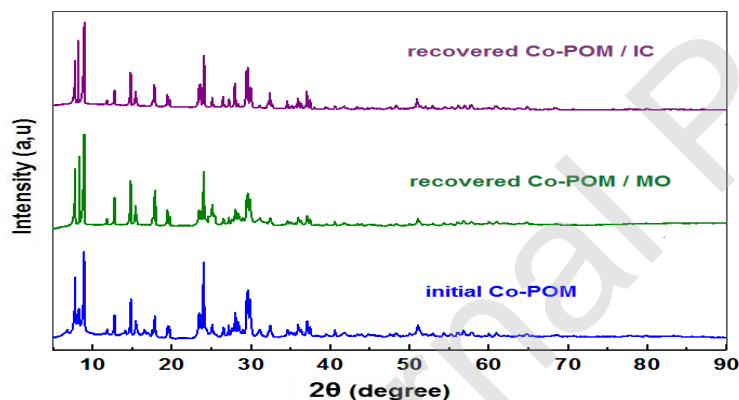
Fig.16. Infra-red spectrums of recovered $P_2W_{17}Co$ (POM) after four cycle of oxidation

Table.3: IR vibration frequencies of recovered polyoxometalates

Compound	vas(P–Oa)	vas(M–Od)	vas(M–Ob–M)	vas(M–Oc–M)
$\alpha_2\text{P}_2\text{W}_{17}\text{Co/IC}$	1087	950	910	759
$\alpha_2\text{P}_2\text{W}_{17}\text{Co/MO}$	1084	946	911	756

3.4.3.X-Ray Diffraction

The recovered catalyst after four oxidation cycles of IC and MO dyes has been characterized by X-ray diffraction, the XRD diffractograms are shown in (Fig.17). According to the diffractograms, the main diffraction angles 2θ are always the characteristics of the Dawson structure [Contant et al.1997; Briand et al.2002], they are observed at (7.7 °, 8.2 °, 8.9 °, 12.6 °, 14.8 °, 17.8 °, 23.9 °, 25.0 °, 25.1 °, 27.8 °, 29.3 °) and (7.7 °, 8.2 °, 8.8 °, 12.8 °, 14.7 °, 17.8 °, 23.8 °, 25.1 °, 25.3 °, 27.6 °, 29.4 °) for the two catalysts (P2W17Co) recovered from the colored solutions of IC and MO respectively. Therefore, the crystalline structure of this Polyoxometalate remains ordered and defined without no change, even in the case of a change in the number of water molecules of crystallization [Ilkenhans et al. 1995; Botto et al.1997].

**Fig.17.** X-Ray diffraction of recovered $\text{P}_2\text{W}_{17}\text{Co}$ (POM) after four test cycle

3.4.4.FE-SEM et EDX analysis

As shown in the (Fig.18), the SEM analysis of the $\text{P}_2\text{W}_{17}\text{Co}$ recovered after the two oxidation reaction of IC (Fig.18.a) and MO (Fig.18.b) did not showed no change in the morphology and microstructure of the catalyst after the four cycles of KMnO_4 oxidation, observing that the catalyst recovered is identical to that of the initial catalyst before use, and that the majority of the nanoparticles still give an aggregate of similar shape to the cubic form with heterogeneous sizes.

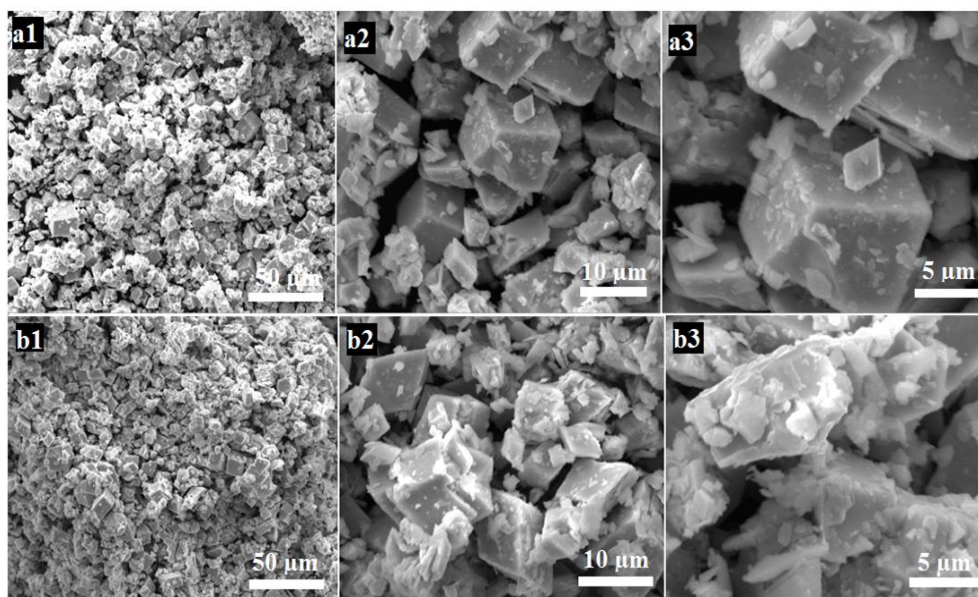


Fig.18. FE-SEM photographs of recovered catalyst after four test cycle at different magnifications : $\alpha_2\text{P}_2\text{W}_{17}\text{Co/IC}$ (a), and $\alpha_2\text{P}_2\text{W}_{17}\text{Co/MO}$ (b)

The EDX spectrograms of the recovered catalysts (Fig.19) also confirm the results obtained according to the SEM analysis, by the presence of the same elements (P, O, K and W) which have already been obtained in the chemical composition of the initial catalyst, presenting always high proportions of tungsten W and oxygen O.

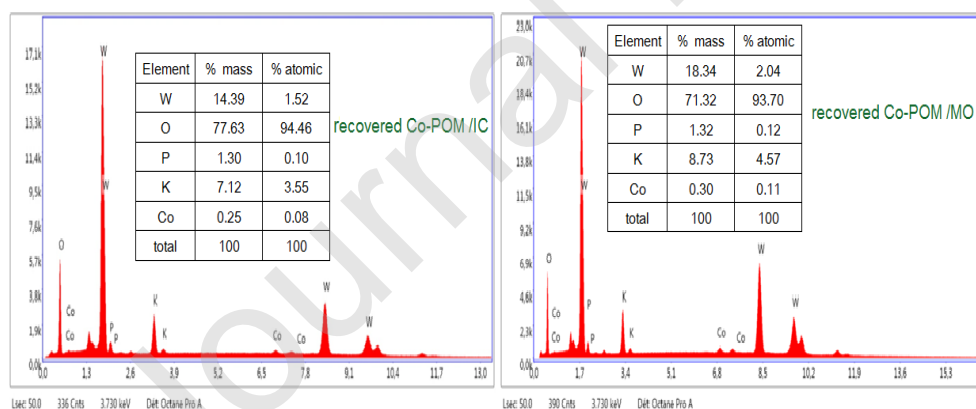


Fig.19. EDX spectra of recovered $\text{P}_2\text{W}_{17}\text{Co}$ (POM) after four test cycle

Finally, the obtained characterizations of recovered catalyst by UV-Vis, FT-IR, DRX, FE-SEM and EDX after four oxidation cycles of MO or IC dyes, confirmed that the catalyst ($\text{P}_2\text{W}_{17}\text{Co}$) is stable and robust [Zabat. 2019], and that the reduction of the discoloration efficiency observed during the four

cycles is not absolutely due to a change in the structure of the recovered catalyst $P_2W_{17}Co$ even if it undergoes several cycles of use.

Conclusion

The separately oxidation of MO and IC by $KMnO_4$ in the presence of a synthesized Nano-POM ($\alpha_2P_2W_{17}Co$)⁸⁻ as catalyst was carried out.

The FT-IR, UV-visible, XRD, FE-SEM and EDX analyses confirmed the structure of Wells-Dawson for the three prepared POMs, specifically the mono-substituted catalyst ($\alpha_2P_2W_{17}Co$)⁸⁻.

The comparison between the two dyes studied revealed that the catalytic oxidation in the aqueous solutions of an indigo dye (IC) and an azo dye (MO) could be carried out under the same operating conditions, especially in an acidic medium and ambient temperature. However, indigo carmine (ED = 75.4%) is more effective than orange methyl (ED = 66.1%) during 60 min.

The spectral evolution over time showed a gradual disappearance of the indigo $-C=C$ band of (IC) and the azo band $N=N$ of (MO) responsible for the color, thus confirming the degradation of these dyes.

The use of different Dawson-structured POMs as catalysts showed a variation in the decolorization efficiency of MO and IC due to the change in the nature of substituted metal, again confirming that Co-substituted ($\alpha_2P_2W_{17}Co$)⁸⁻ is the best catalyst.

The study of catalyst ($\alpha_2P_2W_{17}Co$)⁸⁻ activity and stability has shown its useful life after four cycles. However, as a result, with time, its activity and its effect on the discoloration of dyes reduced gradually. Therefore, to recover and recycle catalyst from these aqueous solutions is very important and significant. The analytical methods FT-IR, UV-visible, XRD, FE-SEM and EDX confirmed the stability and robustness of this recovered catalyst after the fourth oxidation cycle. Thus, this environmental nanomaterial can be considered as a promising catalyst for the treatment of toxic organic pollutants in the colored wastewater.

Conflicts of interest

The authors declare that they have no competing interests.

Acknowledgments

The authors thank the Ministry of Higher Education and Scientific Research, Algeria for the financial support through the PRFU project (N°: A16N01UN230120180001).

References

- Abou-Gamra, Z.M., 2014. Kinetic and Thermodynamic Study for Fenton-Like Oxidation of Amaranth Red Dye. *Adv. Chem. Eng. Sci.* 4, 285-291.
- Alaei, M., Mahjoub, A.R., Rashidi, A., 2012. Effect of WO_3 Nanoparticles on Congo Red and Rhodamine B Photo Degradation. *Iran. J. Chem. Eng.* 31, 23-29.
- Aleboyeh, A., Olya, M.E., Aleboyeh, H., 2009. Oxidative treatment of azo dyes in aqueous solution by potassium permanganate. *J. Hazard Mater.* 162, 1530-1535.
- Ana de Urzedo, P. F. M., Nascentes, C.C., Diniz, M. E. R., Catharino, M.R., Neberlin, R., Rodinei, A., 2007. Indigo Carmine degradation by hypochlorite in aqueous medium monitored by electrospray ionization mass spectrometry. *Rapid. Commun. Mass Spectrom.* 21, 1893–1899.
- Azmat, R., Mohammed, F.V., Ahmed, T., Tanwir, Q-u-A., 2011. Pre-oxidative catalytic treatment of toluidine blue with potassium permanganate in acidic solution. *Front. Chem. China*, 6, 84-90.
- Azmat, R., Yasmeen, B., Uddin, F., 2007. Kinetics of Methylene Blue Reduction with Oxalic Acid by Visible Spectrophotometric Method. *Asian J. Chem.* 19, 1115-1121.
- Bartis, J., Dankova, M., Lessmann, J.J., Luo, Q-H., Horrocks, Jr.W.D., Francesconi, L.C., 1999. Lanthanide Complexes of the α -1 Isomer of the $[\text{P}_2\text{W}_{17}\text{O}_{61}]^{10-}$ Heteropolytungstate: Preparation, Stoichiometry, and Structural Characterization by ^{183}W and ^{31}P NMR Spectroscopy and Europium(III) Luminescence Spectroscopy. *Inorg. Chem.* 38, 1042-1053.
- Bhakya, S., Muthukrishnan, S., Sukumaran, M., Muthukumar, M., Senthil Kumar, T., Rao, M.V., 2015. Catalytic Degradation of Organic Dyes using Synthesized Silver Nanoparticles: A Green Approach. *J. Bioremed. Biodeg.* 6, 312-316.
- Botto, I.L., Cabell, C.I., Thomas, H.J., 1997. $(\text{NH}_4)[\text{TeMo}_6\text{O}_{24} \cdot 7\text{H}_2\text{O}]$ Anderson phase as precursor of the $\text{TeMo}_5\text{O}_{16}$ catalytic phase: thermal and spectroscopic studies. *Mater. Chem. Phys.* 47, 37-45.
- Briand, L.E., Valle, G.M., Thomas, H.J., 2002. Stability of the phospho-molybdic Dawson-type ion $\text{P}_2\text{Mo}_{18}\text{O}_{62}$ in aqueous media. *J. Mater. Chem.* 12, 299-304.
- Bu, L., Shi, Z., Zhou, S., 2017. Enhanced degradation of Orange G by permanganate with the employment of iron anode. *Environ. Sci. Pollut. Res.* 24, 388-394.
- Campos, R., Kandelbauer, A., Robra, K., Cavaco-Paulo, A., Gubitz, G.M., 2001. Indigo Degradation with Purified Laccases from *Trametes hirsuta* and *Sclerotium rolfsii*. *J. Biotech.* 89, 131-139.
- Contant, R., Ciabrini, J.P., 1977. Préparation et propriétés des solutions de quelques hétéropolyanions lacunaires dérivés des 18- tungsto-2-phosphates (isomères α et β). *J. Chem. Res.* 222, 2601-2609.

- Contant, R., Abbessi, M., Canny, J., 1997. Iron-Substituted Dawson-Type Tungstodiphosphates: Synthesis, Characterization, and Single or Multiple Initial Electronation Due to the Substituent Nature or Position, *Inorg. Chem.* 36, 4961-4967.
- Crini, G., 2008. Kinetic and equilibrium studies on the removal of cationic dyes from aqueous solution by adsorption onto a cyclodextrin polymer. *Dyes Pigments.* 77, 415-426.
- Damm, J.H., Hardacre, C., Kalin, R.M., Walsh, K.P., 2002. Kinetics of the oxidation of methyl tert-butyl ether (MTBE) by potassium permanganate. *Water. Res.* 36, 3638-3646.
- De Souza Silva, P.T., Lins da Silva, V., de Barros-Neto, B., Simonnot, M-O., 2009. Potassium permanganate oxidation of phenanthrene and pyrene in contaminated soils, *J. Hazard. Mater.* 168, 1269-1273.
- Devi, G.L., Kumar, S.G., Reddy, K.M., Munikrishnappa, C., 2009. Photo degradation of methyl orange an azo dye by advanced Fenton process using zero valent metallic iron: influence of various reaction parameters and its degradation mechanism. *J. Hazard. Mater.* 164, 459-46.
- Doré, M., 1989. *Chimie des oxydants et traitement des eaux.* TEC. DOC. Lavoisier (editeur), Paris, France, 50.
- El-Ashtoukhy, El-S.Z., 2013. Removal of Indigo Carmine Dye from Synthetic Wastewater by Electrochemical Oxidation in a New Cell with Horizontally Oriented Electrodes. *Int. J. Electrochem. Sci.* 8, 846 – 858.
- Fleischmann, C., Lievenbrück, M., Ritter, H., 2015. Polymers and Dyes: Developments and Applications, *Polymers.* 7, 717-746.
- Hassaan, M.A., El Nemr, A., 2017. Health and Environmental Impacts of Dyes: Mini Review. *Am. J. Environ. Sci. Eng.* 1, 64-67.
- Hill, C.L., Kholdeeva, O.A., 2013. "Selective liquid phase oxidations in the presence of supported polyoxometalates," in *Liquid Phase Oxidation via Heterogeneous Catalysis Organic Synthesis and Industrial Applications*, eds M.G. Clerici, and O. A. Kholdeeva (Hoboken, NJ: John Wiley and Sons, Inc) 263-319.
- Ilkenhans, Th., Hezog, B., Braun, Th., Schlög, R., 1995. The Nature of the Active Phase in the Heteropolyacid Catalyst $H_4PvMo_{11}O_{40}.32H_2O$ Used for the Selective Oxidation of Isobutyric Acid. *J. Catal.* 153, 275-292.
- Inam, U., Shaukat, A., Muhammad, A., 2013. Degradation of Reactive Black B dye in wastewater using oxidation process. *Int. J. Chem. Biochem. Sci.* 4, 96-100.
- Jarrah, A., Farhadi, S., 2019. Dawson-Type Polyoxometalate Incorporated into Nanoporous MIL-101(Cr): Preparation, Characterization and Application for Ultrafast Removal of Organic Dyes. *Acta Chim. Slov.* 66, 85-102.
- Kumar, G., Kumar, R., Hwang, S.W., Umar, A., 2014. Photocatalytic Degradation of Direct Red-23 Dye with ZnO Nanoparticles. *J. Nanosci. Nanotechnol.* 14, 7161-716.

- Li, L., Pengtao, M., Jingping, W., Jingyang, N., 2013. A new inorganic 2D network polyoxometalate constructed from Wells–Dawson phosphomolybdate linked through Cu (II) ions. *Inorg. Chem. Commun.*, 34, 23-26.
- Li-Hong, Y., Yu-Jun, W., Lan, L., Yue-Hua, Z., 2016. Univariate Degradation of Indigo Carmine in Aqueous Solution by Inactivated Biomass in *Heterobasidion Insulare*: Preliminary Studies, *Pol. J. Environ. Stud.* 25, 2221-2225.
- Liu, H., Guo, W., Li, Y., He, S., He, C., 2018. Photocatalytic degradation of sixteen organic dyes by TiO_2/WO_3 -coated magnetic nanoparticles under simulated visible light and solar light. *J. Environ. Che. Engi.* 6, 59-67.
- Long, D-L., Cronin, L., 2012. Pushing the frontiers in polyoxometalate and metal oxide cluster science, *Dalton Trans.* 41, 9815-9816.
- Mahmoodi, N.M., Oveisi, M., Asli, M.A., Rezvani, M.A., Valipour, A., 2017. Bi-aminosurface functionalized polyoxometalate nanocomposite as an environmentally friendly catalyst, synthesis and dye degradation. *Water. Sci. Techn.* 75, 2381-2389.
- Massart, R., Contant, R., Fruchart, J.M., Ciabrini, J.P., Fournier, M., 1977. ^{31}P NMR studies on molybdc and tungsti Polyoxometalates. correlation between structure and chemical shift. *Inorg. Chem.* 16, 2916-2921.
- Neppolian, B., Choi, H.C., Sakthive, S., Arabindoo, B., Murugesan, V., 2002. Solar/UV-induced photocatalytic degradation of three commercial textile dyes. *J. Hazard. Mater* 89, 303-317.
- Olya, M.E., Aleboyeh, H., Aleboyeh A., 2012. Decomposition of a diazo dye in aqueous solutions by $\text{KMnO}_4/\text{UV}/\text{H}_2\text{O}_2$ process. *Prog. Color. Colo. Coat.* 5, 41-46.
- Omwomaa, S., Chen, W., Tsunashima, R., Song, Y-F., 2014. Recent advances on polyoxometalates intercalated layered double hydroxides: From synthetic approaches to functional material applications. *Coord. Chem. Rev.* 258-259, 58-71.
- Ortiz, E., Gómez-Chávez, V., Cortés-Romero, C.M., Solís, H., Ruiz-Ramos, R., Loera-Serna, S., 2016. Degradation of Indigo Carmine Using Advanced Oxidation Processes: Synergy Effects and Toxicological Study. *J. Environ. Protection.* 7, 1693-1706
- Pandey, R., Sisodiya, S., Bende, N., Chourey, V.R., 2014. A Comparative Study of Kinetics of Oxidation of Isoamyl Alcohol and Isobutyl Alcohol by Acidic Permanganate. *Chem. Sci. Rev. Lett.* 3, 658-665.
- Parshetti, G.K., Kalme, S.D., Gomare, S.S., 2007. Biodegradation of reactive blue-25 by *Aspergillus ochraceus* NCIM-1146. *J. Biotechnol.* 98, 3638-3642.
- Pope, M.T, A., 2001. Muller (Eds.), *Polyoxometalate Chemistry: From Topology via Self-Assembly to Applications*, Kluwer, Dordrecht, The Netherlands,

- Qian, X.Y., He, Z.Q., Wu, Q.Y., Tong, X., Yan, W.F., Gong, J., 2011. Synthesis and conductivity of substituted heteropoly acid with Dawson structure $H_7[Ga(H_2O)P_2W_{17}O_{61}]18H_2O$, Chin. Sci. Bull. 56, 2327-2330.
- Ramya, M., Anusha, B., Kalavathy, S., 2008. Decolorization and biodegradation of Indigo carmine by a textile soil isolate *Paenibacillus* larvae. Biodegradation. 19, 283-291.
- Ratna, B., Padhi, S., 2012. Pollution due to synthetic dyes toxicity and carcinogenicity studies and remediation. Int. J. Environ Sci. 3, 940-955.
- Razi Khan, S., Ashfaq, M., Mubashir, Masood, S., 2016. Oxidation Kinetics of Crystal Violet by Potassium Permanganate in Acidic Medium. Russ. J. Phys. Chem. A. 90, 955-961.
- Reza, K.M., Kurny, A., Gulshan, F., 2016. Photocatalytic Degradation of Methylene Blue by Magnetite+ H_2O_2 +UV Process. Int. J. Environ. Sci. Dev. 7, 325-329.
- Rezaee, A., Ghaneian, M.T., Khavanin, A., Hashemian, S.J., Moussavi, Gh., Ghanizadeh, Gh., Hajizadeh, E., 2008. Photochemical oxidation of reactive blue 19 dye (RB19) in textile wastewater by UV/ $K_2S_2O_8$ process. Iran J. Environ. Health Sci. Eng. 5, 95-100.
- Rocchiccioli-Deltcheff, C., Thouvenot, R., 1979. Vibrational studies of Polyoxometalates related to $\alpha-P_2W_{18}O_{62}^{6-}$. Spectrosc. Lett. 12, 127-138.
- Schwegler, M.A., 1991. Heteropolyacids Catalysts in Organic Reactions (PhD thesis), Delft University of Technology, Netherland.
- Secula, M.S., Cretescu, I., Petrescu, S., 2011. An experimental study of indigo carmine removal from aqueous solution by electrocoagulation, Desalination. 277, 227-235
- Shojaei, A.F., Rezvani, M.A., Heravi, M., 2011. A green, reusable and highly efficient solid acid catalyst for the oxidation of aldehydes to the corresponding carboxylic acids using H_2O_2 and $KMnO_4$: $H_5PV_2Mo_{10}O_{40}$ (10-molybdo-2-vanadophosphoric heteropolyacid). J. Serb. Chem. Soc. 76, 1513-1522.
- Si, L., Wei, Y., Chenglong, C., Yanbo, W., Shuangchun, Y., 2013. Research progress of the physical and chemical treatment of dye wastewater. Int. J. Sci. Eng Res. 4, 2010-2012.
- Song, Y.F., Tsunashima, R., 2012. Recent advances on polyoxometalates based molecular and composite materials. Chem. Soc. Rev. 41, 7384-7402.
- Troupis, A., Gkika, E., Triantis, T., Hiskia, A., Papaconstantinou, E., 2007. Photocatalytic reductive destruction of azo dyes by polyoxometallates: Naphthol blue black. J. Photochem. Photobiol. A: Chem. 188, 272-278.
- Troupis, A., Triantis, T.M., Gkika, E., Hiskia, A., Papaconstantinou, E., 2009 Photocatalytic reductive-oxidative degradation of Acid Orange 7 by polyoxometalates. Appl. Catal. B. Environ. 86, 98-107.

- Vella P.A., Munder J.A., 1993. Toxic pollutant destruction comparison of the oxidants potassium permanganate, Fenton reagent, and chlorine dioxide on the toxicity of substituted phenols, ACS. Symp. Ser. 518, 85-105.
- Wang, W., Yang, S., 2010. Photocatalytic degradation of organic dye methyl orange with phosphotungstic acid. J. Water Resour. Prot. 2, 979-983.
- Xiang-Rong, X., Hua-Bin, L., Wen-Hua, W., Ji-Dong, G., 2005. Decolorization of dyes and textile wastewater by potassium permanganate, Chemosphere. 59, 893-898.
- Xiao, Z., Chen, K., Wu, B., Li, W., Wu, P., Wei, Y., 2016. An easy way to construct polyoxovanadate-based organic-inorganic hybrids by stepwise functionalization. Eur. J. Chem. 2016, 808-811.
- Yan, Y.E., Schwartz, F.W., 1999. Oxidative degradation and kinetics of chlorinated ethylenes by potassium permanganate. J. Contam. Hydrol. 37, 343-365.
- Yan, Y.E., Schwartz, F.W., 2000. Kinetics and mechanisms for TCE oxidation by permanganate, Environ. Sci. Technol. 34, 2535-2541.
- Yoshioka, N., Ichihashi, K., 2008. Determination of 40 synthetic food colors in drinks and candies by highperformance liquid chromatography using a short column with photodiode array detection. Talanta. 74, 1408-1413.
- Zabat, N., Abbess, M., 2015. Elimination of the methyl blue from wastewater by advanced oxidation process in the presence of an heteropolyanion of Dawson type as a catalyst, Res Chem Intermed. 41, 1691-1702.
- Zabat, N., 2018. Comparative study of discoloration of mono-azo dye by catalytic oxidation based on wells-dawson Polyoxometalate catalyst, Environ. Nanotechnol. Monit. Manage. 10, 10-16.
- Zabat, N., 2019. Nickel-Substituted Polyoxometalate Nanomaterial as a Green and Recyclable Catalyst for Dye Decolorization. Arab. J. Sci. Eng. 44, 227-236.